In Situ X-ray Scattering Study of a Model Thermotropic Copolyester under Shear: Evidence and Consequences of Flow-Aligning Behavior

V. M. Ugaz and W. R. Burghardt*

Department of Chemical Engineering, Northwestern University, Evanston, Illinois 60208

Received July 31, 1998

ABSTRACT: While director tumbling is responsible for much of the unique rheological behavior of *lyotropic* liquid-crystalline polymers (LCPs), it is not clear whether tumbling routinely occurs in main-chain thermotropes. We present experiments on a model thermotropic LCP under shear, using in-situ X-ray scattering as a probe of molecular orientation. This model LCP, PSHQ6−12, was synthesized by Chang and Han [*Macromolecules* **1996**, *29*, 2383] and consists of rigid mesogens randomly copolymerized with flexible spacer chains of two different lengths. This architecture suppresses crystallization and lowers the nematic−isotropic transition temperature to an accessible level, allowing a well-defined thermal history to be established prior to flow. We present measurements of molecular orientation in steady shear flow, during relaxation, and during shear flow start-up. The evolution of molecular orientation observed during flow inception and the observation of shear-induced transparency in the material lead to the hypothesis that PSHQ6−12 is shear aligning rather than tumbling. Consequences of this hypothesis are explored by polydomain simulations based on Ericksen's transversely isotropic fluid model, which are capable of capturing many aspects of the experimentally observed rheology and shear-induced structure.

1. Introduction

Technological interest in liquid-crystalline polymers (LCPs) is driven by their combination of low-weight, high-temperature stability and exceptional mechanical strength. Since mechanical properties are strongly influenced by the high degree of molecular alignment possible in LCPs, an understanding of the effect of flow on molecular orientation is essential in order to better control the processing conditions which give rise to and enhance these properties. Development of a consistent theoretical description of LCP rheology has proven to be a complex and challenging undertaking. To date, model lyotropic systems have been the primary focus of study, and there has been considerable success in rationalizing their rheological behavior using concepts from continuum, molecular, and mesoscopic polydomain models. These theories are reviewed by Marrucci and Greco[1] and can successfully predict many of the unique rheological phenomena observed in lyotropic systems, including negative values of the steady-state first normal stress difference,[2] oscillations in shear and normal stress following step changes in shear rate,[3] and large elastic recovery during constrained recoil.[4]

As expected in any material possessing a complex microstructure, a strong connection exists between structure and rheology in LCPs. On a local level, material response is expressed in terms of the *director,* a unit vector indicating the direction of average molecular orientation in the nematic phase. Continuum theory predicts that nematics may respond to shear in two distinct ways in the linear limit (i.e., when shear does not perturb the local molecular order parameter). In the case of a *flow-aligning* material, hydrodynamic torques on the director disappear when it assumes a characteristic alignment angle with respect to the shear flow direction. For some materials, however, it is possible that no alignment angle brings hydrodynamic torques into balance. In the absence of other torques, this imbalance leads to indefinite rotation of the director—a condition known as *director tumbling*. Director tumbling has been directly confirmed in various lyotropic systems through experiments on monodomain samples[5−7] and lies at the heart of most unique rheological phenomena observed in lyotropic LCPs. In the low shear rate linear regime, tumbling provides a direct explanation for stress oscillations observed in transient flows. Damping of these oscillations is attributed to elastic effects associated with spatial distortions of the director field induced by tumbling. This *distortional elasticity* also provides the driving force for large strain recovery.[8,9] Director tumbling in the linear limit is correctly predicted by the Doi model,[10] provided certain mathematical approximations are avoided.[11] A regime of negative normal stresses is then predicted to be a signature of a transition from tumbling to aligning behavior induced by nonlinear viscoelastic effects.[12,13] Director tumbling and the associated nonlinear transition to flow alignment also impact the bulk orientation state in sheared LCPs. Birefringence,[14−17] X-ray scattering,[17−22] and neutron scattering[23−25] have been useful for quantitative measurements of molecular orientation, providing additional insights into the relationship between orientation and rheology in lyotropic LCPs.

Lyotropic LCP rheology is currently much better understood than that of main-chain thermotropic systems. In particular, the basic question of whether thermotropes exhibit tumbling or flow alignment during shear has not been clearly resolved. This issue has been directly addressed in only a single set of monodomain experiments on a model main-chain polymer with rigid mesogens separated by flexible spacers.[26] In this material, flow alignment was observed close to T_{NI} (the nematic−isotropic transition temperature), while tumbling was found close to a nematic−smectic phase transition. For most thermotropes, only indirect evidence of tumbling or flow alignment is available. In

* Corresponding author: w-burghardt@nwu.edu. Phone: 847-467-1401. Fax: 847-491-3728.

10.1021/ma981215k CCC: $15.00
Published on Web 11/10/1998

lyotropes, the most reliable signatures of tumbling are the presence of negative normal stresses in steady shear and stress oscillations in transient shear flows. To provide a context for our work, we next review relevant observations in thermotropes.

Two classes of main-chain thermotropic LCPs have been studied extensively. The first is commercial copolyesters, where semiflexible backbones and chemical irregularity along the chain suppress the crystal melting point, thereby producing an accessible nematic phase.[27] Well-defined experiments with these materials are challenging since T_{NI} is usually inaccessible, making it impossible to erase the effects of previous thermal and shear history. In addition, recrystallization[28] and transesterification[29] can occur at melt temperatures, leading to time-dependent material properties. The other broad class of main-chain thermotropic LCPs consist of rigid mesogenic units separated by flexible hydrocarbon spacers. By lowering transition temperatures, this architecture makes the isotropic phase accessible, thereby making it easier to conduct well-controlled rheological experiments. We thus refer to such materials as "model" thermotropic LCPs.

There have been no reproducible reports of a steady negative first normal stress difference in thermotropic LCPs. Early reports of negative N_1 in commercial copolyesters appear to have been undermined by residual normal stresses associated with sample loading.[30,31] An investigation comparing commercial and model LCPs reveals the advantages of an accessible isotropic phase in establishing well-defined initial conditions for rheological testing.[32] Han and co-workers have performed extensive rheological studies on model thermotropic polyesters denoted PSHQ*n*, where "*n*" indicates the number of carbons in the flexible spacer (e.g. PSHQ10 = poly[(phenylenesulfonyl)-*p*-phenylene 1,10-decamethylenebis(4-oxybenzoate)]). Their most extensive studies have been on PSHQ10,[33−35] and have also included studies on the effects of molecular weight[36] and flexible spacer length[37,38] on shear rheology. In all cases, positive N_1 values were observed in steady shear.

The lack of negative N_1 values in steady shear does not, however, prove that tumbling is absent. Magda and co-workers have performed detailed studies of a first normal stress difference in hydroxypropylcellulose [HPC] solutions over a very wide concentration and temperature range, almost reaching the thermotropic limit (pure polymer).[39,40] At fairly low concentrations in the liquid-crystalline state, a sequence of N_1 sign changes conforms to the theoretically predicted transition from tumbling to flow alignment.[13] At higher concentrations, a relative minimum is still observed in N_1 as a function of shear rate, but N_1 remains positive. It is suggested that the underlying dynamics continue to exhibit a transition from tumbling to alignment, but that additional viscous stresses neglected in the original Doi model are generated by the tight packing of molecules.[39] In their most recent work, Magda and co-workers reported a local minimum in N_1 at HPC concentrations as high as 70 wt %. In addition, negative N_1 values were observed in lower concentration solutions at high temperatures where HPC forms a thermotropic phase.[40] While not definitive, these results suggest this semiflexible molecule may continue to exhibit tumbling in its thermotropic phase. The types of relative minima reported by Magda and co-workers have typically not been observed in either model or commercial thermotropic LCPs, although such data are often restricted to narrow shear rate ranges.

Another typical signature of tumbling is oscillatory stress responses in transient flows. The most commonly studied flow in thermotropes is start-up of steady shear. In commercial LCPs, the deformation applied during sample preparation and loading will have a large effect on start-up behavior. While reproducible results may be obtained by following identical sample preparation protocols,[41] the ill-defined initial condition makes interpretation of start-up transients difficult and inhibits meaningful comparisons of experiments from different groups. In model LCPs, initial conditions may be reproducibly generated by heating the sample into the isotropic phase; subsequent cooling into the nematic phase results in a polydomain structure with no net orientation. Start-up experiments on PSHQ10[33] and a very similar fluorinated derivative[42] both show large shear stress overshoots and weak negative N_1 undershoots followed by more pronounced overshoots. However, in studies of PSHQ6−12 (a random copolymer incorporating two spacer lengths), Chang and Han do not report any negative N_1 transients.[37] At lower temperatures and higher rates, multiple overshoots are observed in N_1, while multiple overshoots in shear stress are less common.[33,42] Although multiple overshoots could be taken as a signature of tumbling, they have more typically been attributed to the transient response at different structural levels.[41,42] Using step-change protocols similar to those introduced by Mewis and Moldenaers,[3] Beekmans and co-workers[43] obtained nicely reproducible transients in a commercial thermotrope that resemble those observed in tumbling lyotropes. However, under most circumstances, stress transients in thermotropes do not exhibit the characteristic damped oscillations that are taken as a clear indication of tumbling.

In situ studies of the fluid structure are also less common in thermotropes, as compared to lyotropic LCPs. The strong turbidity of thermotropes renders optical techniques much more difficult to apply. Mackley and co-workers have studied disclination line dynamics in sheared commercial thermotropes using optical microscopy on very thin samples;[44,45] however, it is not clear how these observations relate to rheology or orientation in bulk melts. Aromatic copolyesters under shear have been studied by X-ray scattering,[46,47] and transitions in the orientation state as a function of temperature and shear rate have been reported.[47] However, it appears these transitions may be related to residual ordering in the melt state, a typical concern with commercial LCPs.[28] Since rheological data may be more reliably obtained on model thermotropes, it is sensible to perform structural studies using these systems as well. As an example, optical microscopy on sheared PSHQ10 has supported mechanical rheological evidence of flow-induced shifts in T_{NI}.[48]

In this paper, we report a study of molecular orientation in the model thermotropic LCP PSHQ6−12, using X-ray scattering. The mechanical rheology of this material has previously been studied in great detail by Chang and Han,[37] providing a context for the interpretation of structural data. Of particular interest is whether the results of this study provide any indication of the tumbling or flow-aligning character of this material in shear. Various observations suggest that PSHQ6−12 is a flow-aligning nematic. The consequences of this

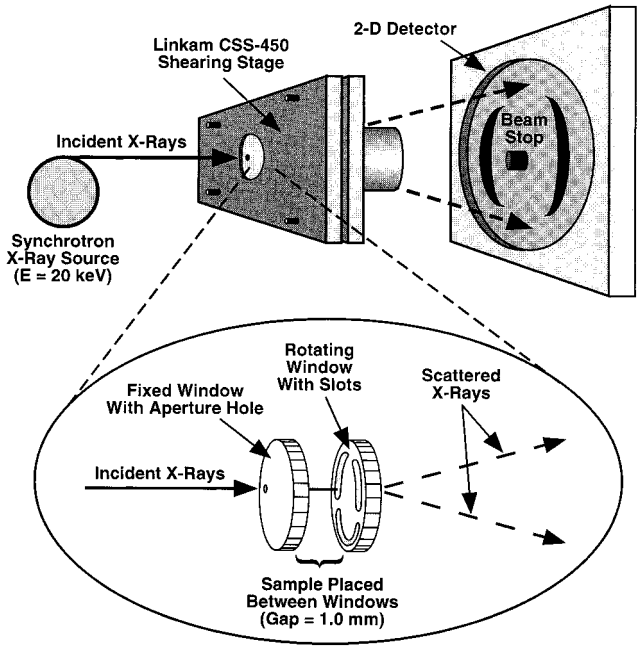

Figure 1. Schematic illustration of the X-ray shearing cell setup. The exploded view depicts the shearing geometry and window design which allows the X-ray beam to pass through the sample during shear. Drawing is not to scale.

possibility are then considered further using a simple model to calculate how macroscopic orientation should evolve under shear from an initially random polydomain, and the associated mechanical response.

2. Experimental Section

2.1. Materials. The material used in this study is PSHQ6−12, a main-chain thermotropic copolyester incorporating flexible spacers of two different lengths (6 and 12 CH_2 units) randomly distributed along the polymer backbone. The sample was synthesized using procedures described elsewhere,[49] and generously provided by Professor C. D. Han. The copolymer architecture suppresses both smectic and crystalline phases and leads to a broad nematic phase from 90 to 190 °C. In fact, crystallization is completely suppressed and PSHQ6−12 is a glassy solid, thus avoiding all possible complications of recrystallization in the nematic phase.

Samples were prepared by solvent casting following a protocol similar to that detailed by Chang and Han.[37] Films were cast from a solution in dichloromethane (Fisher Scientific) in the presence of the antioxidant Irganox 1010 (Ciba-Geigy). All materials were used as received. The as-cast films were further dried in a vacuum oven and then cut into disks sized to fit inside the shearing cell. In their differential scanning calorimetry analysis of PSHQ6−12 during heating scans at a rate of 20 °C/min, Chang and Han[49] observed two thermal transitions: a glass transition at 92 °C and a nematic−isotropic transition at 193 °C whose exothermic peak spans a temperature range of approximately ±5−10 °C. The sample had a weight-average molecular weight of 24300 with a polydispersity of 2.02.[49]

2.2. Experimental Setup. A Linkam CSS-450 high-temperature shearing stage was modified for X-ray scattering by replacing the quartz optical windows with suitable X-ray windows as shown in Figure 1. The unit provides a parallel disk-shearing geometry, and stainless steel inserts were used to support the X-ray windows. An aperture hole located in the fixed plate defines the incident beam size. The rotating window incorporates slots at the same radius as the aperture hole that are wider than the beam, allowing all scattering up to angles of $2\theta = 14°$ from the illuminated sample to emerge from the flow cell. Thin sheets of either mica or Kapton were glued to the surface of each disk to serve as the actual X-ray window material. This flow cell is similar to a device constructed in our group for room-temperature X-ray scattering experiments in lyotropic LCPs,[20] which is in turn modeled after a parallel plate X-ray flow cell described by Keates and coworkers.[19]

Two-dimensional scattering patterns were collected using either image plates (steady-shear and relaxation experiments) or a wire grid position sensitive detector (flow-inception experiments). The combination of synchrotron radiation and the wire grid detector provided sufficient time resolution for transient flow phenomena to be readily observed during flow inception. Scattering experiments were conducted on beamline 5-BM at the Advanced Photon Source (APS) of Argonne National Laboratory. In all X-ray experiments, the sample thickness was 1 mm, and the energy of the incident radiation was 20 keV ($\lambda = 0.621$ Å). Use of fairly high energy confines the wide-angle scattering from our LCP sample to smaller angles; this ensures that the scattered radiation corresponding to the structural features of interest is not blocked by the flow cell.

We followed thermal-clearing protocol identical to that used by Chang and Han[37] in their rheological studies of this material in order to ensure that a stable and reproducible initial morphology was attained in all experiments. This protocol involved heating the sample to the isotropic phase (205 °C), shearing for 10 min at a shear rate of 0.1 s^{-1} and then cooling the quiescent sample to the desired temperature in the nematic phase.

A series of optical transmission measurements were also conducted to measure changes in the turbidity of the sample during shear. An advantage of the modified Linkam shearing stage is the ability to perform both optical and X-ray scattering experiments using a single flow cell by installing the appropriate windows. The optical transmission setup consisted of measuring the intensity of a HeNe laser beam transmitted through the sample using a photodiode detector. A sample gap of 400 μm was used for these transmission experiments.

2.3. Data Analysis. The degree of molecular orientation may be quantitatively represented by an orientation parameter, S, whose value ranges from zero, corresponding to the random alignment of molecules, to 1, corresponding to perfect alignment of all molecules along the flow direction. In LCPs, values of S less than 1 reflect imperfect alignment at two levels of structure.[17] First, the local molecular-order parameter (S_m) will be less than 1 because of the imperfect local orientation of the molecules in the nematic phase. Thermodynamic models of LC phase behavior predict increases in S_m with undercooling below the nematic−isotropic transition. Second, LCPs generally exhibit a defect-ridden morphology characterized by a distribution of director orientation. By analogy with polycrystalline solids, LCPs are often described in terms of a "polydomain" texture. The distribution of *director* orientation is sometimes characterized by a mesoscopic order parameter, $\bar{S}$. Consequently, bulk measurements of orientation reflect both levels of structure, in a way which may be qualitatively expressed as

$$S = S_m \bar{S} \tag{1}$$

Experimentally, S is determined from an average of the second Legendre polynomial weighted by an azimuthal intensity scan as shown in eq 2:

$$S \equiv \frac{\langle P_2(\cos\alpha)\rangle}{\langle P_2(\cos\alpha)\rangle_0} = -2\left[\frac{\int_0^{\pi/2} I(q,\alpha)\, P_2(\cos\alpha)\sin\alpha\, d\alpha}{\int_0^{\pi/2} I(q,\alpha)\sin\alpha\, d\alpha}\right] \tag{2}$$

The azimuthal angle α is measured from the flow direction, and q is the scattering vector at which the azimuthal scan is obtained. We have selected q to coincide with the location of the equatorial nematic scattering peak. In eq 2, $\langle\cdots\rangle$ represents

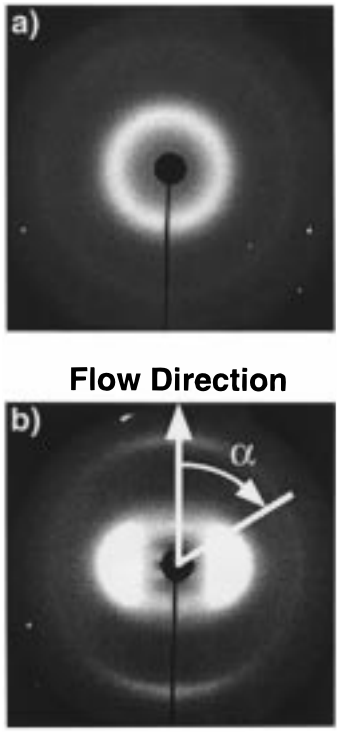

Figure 2. Typical X-ray scattering patterns from PSHQ6-12 (a) after shearing in the isotropic phase (205 °C) at 0.1 s^{-1} for 10 min and (b) under steady shear at 0.05 s^{-1} in the nematic phase (160 °C). In (b), the azimuthal angle α used in eq 2 is defined.

an average weighted by the azimuthal intensity scan $I(q,\alpha)$, while $\langle\cdots\rangle_0$ represents an average weighted by the azimuthal intensity distribution which would be expected for perfect alignment ($S = 1$). Here, we follow Mitchell and Windle,[50] who assume that the scattering objects are infinite rods, and consequently that the azimuthal intensity distribution for perfect alignment corresponds to $\delta(\alpha - \pi/2)$; this leads to the factor of -2 on the right-hand side of eq 2.

3. Experimental Results and Discussion

3.1. Typical Scattering Features. Figure 2 shows representative two-dimensional X-ray scattering patterns in the isotropic and nematic phases. In the isotropic state, the pattern consists of a diffuse ring indicating the absence of any preferred direction of molecular alignment. This pattern is highly reproducible, confirming that the thermal-clearing protocol generates a uniform initial condition. Shearing in the isotropic phase at moderate rates leads to no discernible change in the pattern; shear forces are insufficient to promote significant alignment at the local mesogen length scales probed in these wide-angle scattering measurements. Once a quiescent sample is cooled into the nematic phase, little change is observed in the scattering pattern. Although the mesogens align locally in the nematic phase, there is no preferred global orientation direction. Instead, the sample exhibits a random distribution of director orientations associated with the quiescent "polydomain" state. Calculation of an orientation parameter using eq 2 under these conditions leads to $S = 0$.

When the sample is sheared in the nematic phase (Figure 2b), an anisotropic pattern is generated, characterized by two diffuse equatorial peaks whose radial position is related to an average *inter*molecular correlation distance (d = 5 Å) characteristic of the lateral

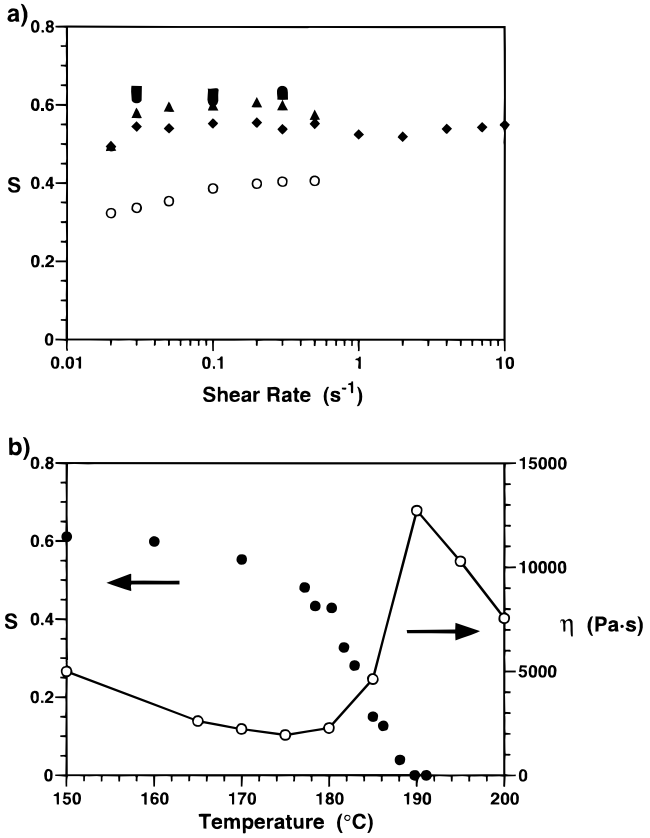

Figure 3. (a) Orientation parameter as a function of shear rate in steady shear flow at 140 °C (■), 150 °C (●), 160 °C (▲), 170 °C (◆), and 180 °C (○). (b) Molecular orientation (●, left ordinate) and viscosity (○, right ordinate; data from ref 37) in steady shear flow at 0.1 s^{-1} as a function of temperature.

packing of molecules in the nematic phase. This is the location where azimuthal scans are taken for the subsequent computation of molecular orientation parameters. In addition, the pattern shows two fainter peaks located on the meridian whose locations are related to an average *intra*molecular correlation length along the polymer backbone (d = 2 Å).

3.2. Orientation in Steady Shear. Figure 3a shows the dependence of molecular orientation on the shear rate and temperature in steady-shear flow. At temperatures well within the nematic phase, the steady-state level of molecular orientation is fairly insensitive to shear rate over the range of rates probed. Furthermore, molecular orientation decreases with increasing temperature. Modest decreases are seen from 140 to 170 °C, while a more dramatic drop is observed between 170 and 180 °C where S falls by almost a factor of 2. In addition, S does increase monotonically with the shear rate at 180 °C.

The drop in orientation at 180 °C can be explained by referring to Figure 3b in which steady-shear values of molecular orientation and viscosity (data from ref 37) are plotted as a function of temperature for a fixed shear rate of 0.1 s^{-1}. In the isotropic phase (T > 190 °C), viscosity increases with decreasing temperature. Upon the formation of a nematic phase, the viscosity drops precipitously, reaching a minimum at T = 175 °C. Comparing the viscosity and orientation parameter, this drop in viscosity is clearly associated with the development of the nematic order. Formation of the ordered phase results in greater local mobility of the molecules, similar to the decrease in viscosity predicted by the Doi

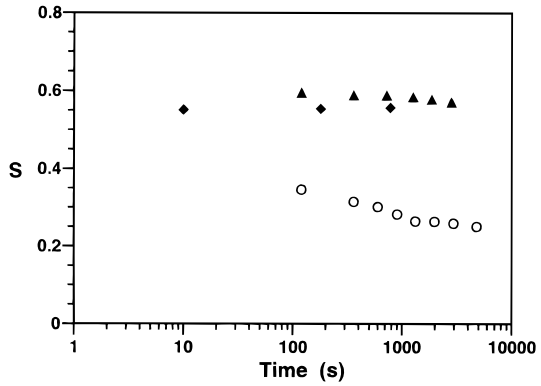

Figure 4. Orientation parameter as a function of time during relaxation from steady shear at a rate of 0.1 s^{-1} at 160 °C (▲), 170 °C (◆), and 180 °C (○).

model upon the formation of the nematic phase with increasing concentration in lyotropes.[10] These data suggest that 180 °C lies inside the biphasic regime between nematic and isotropic states. Chang and Han[37] identified the biphasic nature of the transition region, ranging from approximately 180 to 193 °C, through observation of the domain texture using polarized optical microscopy. They attributed the physical origin of the biphasic regime to the effects of polydispersity. Both rheological and X-ray data suggest that the sample is isotropic at temperatures of 190 °C and above. This is lower than the T_{NI} measured using DSC (193 °C), but that transition temperature was measured using a fairly high heating rate, which likely explains the difference.

The loss of orientation upon clearing was also studied in a sample that had been oriented by shear in the nematic phase, and then heated in the quiescent state through the isotropic−nematic transition. The behavior was virtually identical to that seen in Figure 3b, with the measurable orientation disappearing at 190 °C. These X-ray measurements thus show no effect of shear on the isotropic−nematic transition temperature in PSHQ6−12, at a rate of 0.1 s^{-1}. Mather and co-workers did observe an increase in T_{NI} of 6 °C in PSHQ10 with shear rates around 0.4 s^{-1}.[48] Higher shear rates might also have an effect on the clearing temperature of PSHQ6−12.

3.3. Relaxation upon Shear Flow Cessation. Figure 4 shows the evolution of molecular orientation during relaxation from steady shear at three different temperatures. Well within the nematic phase, molecular orientation does not change appreciably during relaxation up to times of 1 h, and S instead remains at the value generated during the steady-shear flow. As in Figure 3a, the behavior is somewhat different at 180 °C, where orientation is lower, and some relaxation in S takes place. Assuming the sample is biphasic at this temperature, partial relaxation in bulk orientation may be expected due to relaxation of phase boundaries deformed during the prior shear flow.

Chang and Han performed several interrupted shear experiments at 160 °C, using a shear rate of 0.1 s^{-1}.[37] Shear flow inception from a thermally cleared, random polydomain structure resulted in significant stress overshoot peaks (see Figure 5b below). After reaching steady state, the flow was stopped, and then resumed after several different delay times. Upon flow resumption, no shear stress overshoot was observed, even for relaxation times of 3 h. Instead, the previous steady-shear stress was reestablished almost immediately. This

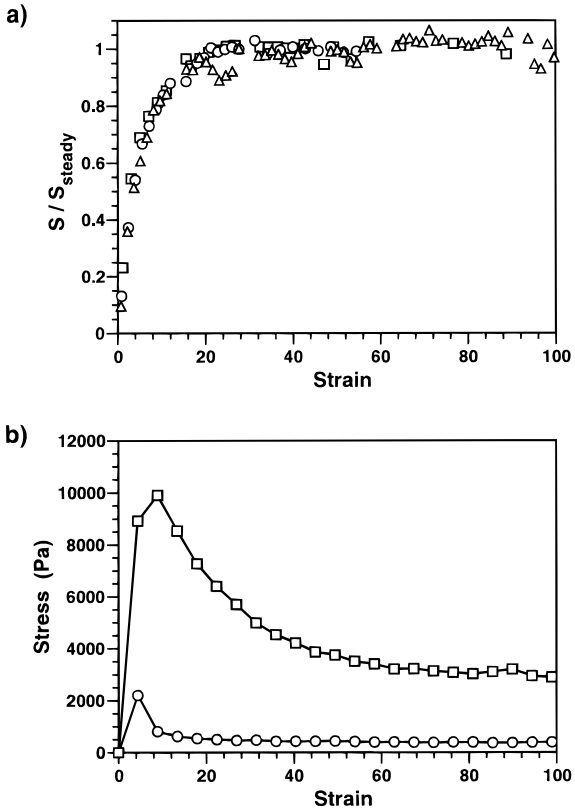

Figure 5. Flow inception in PSHQ6-12 at 160 °C. (a) Evolution of normalized molecular orientation as a function of applied strain during flow start-up at shear rates of 0.03 (□), 0.1 (○), and 0.3 s^{-1} (△). (b) Shear stress (○) and first normal stress difference (□) as a function of applied strain at a rate of 0.1 s^{-1} (data from ref 37).

rheological response is consistent with the data in Figure 4 which show that no significant structural rearrangement occurs during relaxation over the time scales probed in our experiments. Chang and Han did observe some indications of structural relaxation at longer times, in that the first normal stress difference exhibited a weak, but appreciable, overshoot after a delay of 3 h.[37] They attributed the reemergence of this overshoot in N_1 to partial recovery of a polydomain texture. The fact that no shear stress peak was observed after 3 h of relaxation suggests that N_1 is more sensitive to structural recovery than shear stress.

3.4. Shear Flow Inception. Figure 5a shows the evolution of an orientation parameter upon flow start-up at three different shear rates at a temperature of 160 °C. Molecular orientation increases monotonically, approaching a steady-state value within approximately 20 strain units. The data show excellent strain scaling during the start-up transient and lack of any sign of oscillatory behavior. Figure 5b shows shear stress and first normal stress difference data of Chang and Han[37] from a flow inception experiment for PSHQ6−12, also conducted at 160 °C. These results are similar to those obtained at other temperatures,[37] although the magnitude of the stress overshoots can depend on undercooling in the nematic phase. No oscillations were observed in shear stress transients upon flow inception from a thermally cleared initial condition. Weak multiple overshoots in N_1 were observed on flow start-up at temperatures of 160 °C and below; the N_1 data in Figure 5b show an example of a weak second peak. Given that tumbling lyotropes exhibit significant oscillations in

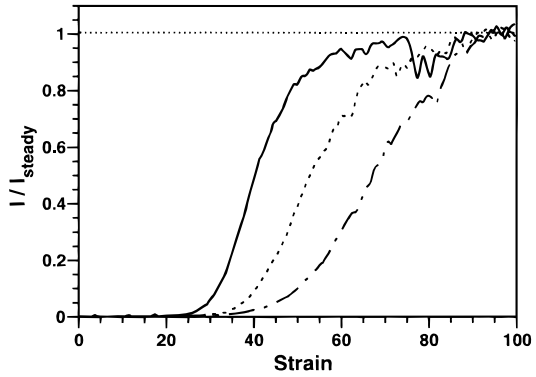

Figure 6. Evolution of normalized transmitted intensity of a HeNe laser beam as a function of applied strain during flow start-up at rates of 0.03 (—), 0.1 (- - -), and 0.3 s^{-1} (—•—). Sample thickness is 400 μm.

both shear and normal stresses[51] which are well-correlated with significant oscillations in bulk orientation,[17] X-ray and mechanical results presented in Figure 5 both seem more consistent with flow-aligning dynamics.

Further evidence of flow-aligning character in PSHQ6−12 is obtained by visual inspection of the sample during shear. When subjected to flow start-up in the nematic phase, the sample undergoes a dramatic transformation from an opaque appearance characteristic of the thermally cleared, random polydomain initial condition, to a quite transparent appearance. The likely explanation for this behavior is that shearing induces sufficiently homogeneous molecular orientation to reduce scattering and render the material optically transparent. Since generation of such a uniform orientation state is difficult to conceive in a tumbling material, this shear induced transparency suggests flow-aligning behavior in PSHQ6−12.

To quantify the shear-induced transparency, we conducted a series of optical transmission experiments. Figure 6 shows the intensity of light from a HeNe laser beam transmitted through the sample during flow start-up at 160 °C. Initially, no light is transmitted due to strong scattering from the random polydomain initial condition. Shear flow is clearly capable of significantly reducing the turbidity of the sample; however the increase in transmittance does not begin until 20−30 strain units have elapsed—strain levels at which the X-ray data indicate that the molecular orientation has saturated at the steady-state value.

The development of transparency may involve a two-step process. Upon flow inception in a flow-aligning material, regions of the sample with initially random director orientations would all evolve toward the flow-alignment angle, reflected in the increase in S observed in the X-ray scattering data (see section 4 below). Evidently, after 20 strain units the sample may be quite well-aligned from the point of view of bulk X-ray measurements, yet still not have achieved sufficient homogeneity to render it optically transparent. While Figure 5a shows that the development of bulk orientation follows strain scaling, the evolution of transmittance in Figure 6 does not scale with applied shear strain. A second, local process of defect elimination or texture refinement may be necessary to achieve sufficient homogeneity to yield significant transparency. Since transparency evolves earliest (as a function of strain) at the lowest shear rate in Figure 6, perhaps this second process occurs on some characteristic time scale which is independent of the applied shear rate, once shear has promoted strong bulk orientation. We attempted in situ optical microscopy experiments using the Linkam shearing stage in our laboratory; however, the combination of magnification limitations and the 400-μm sample thickness obscured details of the defect texture evolution. While use of thinner samples would facilitate microscopy studies, they carry the danger of increased surface effects. With the 400 micron sample thickness, the steady state value of the transmitted intensity in the sheared nematic phase is approximately 60% of the corresponding value in the isotropic phase, indicating that shear is not completely effective in promoting sample transparency.

3.5. Discussion. Given the complex rheological and structural behavior observed in sheared lyotropic LCPs, the data reported here for PSHQ6−12 are comparatively simple, and consistent with the hypothesis that PSHQ6−12 is shear-aligning under the conditions of these experiments. While orientation in lyotropes often is a complex function of shear rate,[17] Figure 3a shows orientation that depends little on the shear rate. For an aligning nematic, shear should promote a unique director orientation, and eq 1 suggests that the bulk orientation parameter should reflect the local molecular ordering. Indeed, Figure 3b shows modest increases in S with undercooling in the nematic phase, as would be expected in the equilibrium molecular order parameter. Measurements in flow inception show no strong indication of the characteristic oscillatory responses characteristic of tumbling in lyotropes, and prolonged shear renders PSHQ6−12 fairly transparent, which would be inconsistent with the heterogeneous orientation state thought to be generated by tumbling.

The assessment of shear-aligning behavior in a main-chain thermotrope by Srinivasarao and co-workers[26] yielded somewhat ambiguous results: they observed shear alignment near T_{NI}, but tumbling at lower temperatures close to a smectic-phase transition. Since proximity to a smectic phase is known to induce tumbling in low-molecular-weight liquid crystals, it is reasonable to attribute the tumbling in their study to similar physics. While PSHQ6−12 has a chain architecture similar to the sample studied by Srinivasarao et al. (mesogen/flexible spacer), mixing two widely separated spacer lengths inhibits smectic-phase formation. Thus, shear-aligning behavior in PSHQ6−12 is consistent with this limited literature data.

Since molecular models give insights into the origins of tumbling behavior in rigid-rod lyotropic solutions, it is also informative to consider any guidance available from molecular models applicable to thermotropes. In general, thermotropic main-chain LCPs have greater flexibility than lyotropes. The influence of chain flexibility on the shear-aligning tendency of semiflexible, nematic polymers is apparently complex. Greco and Marrucci[52] investigated the effects of slight flexibility in the Doi model and found that it *increased* the propensity toward tumbling in the low-shear-rate limit. Conversely, the limit of high flexibility was shown by Semenov[53] to lead to flow-aligning behavior. A related prediction was made by Maffettone and Marrucci,[54] who formulated a simple rheological model for a nematic freely jointed chain (the nematic dumbbell model) which also predicts flow-alignment in shear at all shear rates.

The presence of flexible spacers in model main-chain thermotropic LCPs should render them very flexible; indeed, the model adopted by Maffettone and Marrucci seems particularly well-suited for this chain architecture. It is then gratifying that the direct measurements of Srinivasarao et al.[26] and the indirect evidence presented here are in apparent agreement with this prediction of flow alignment. Thermotropic HPC or commercial copolyesters, however, have less intrinsically flexibility, and it is quite possible that these materials may exhibit tumbling, as suggested by the experiments of Magda and co-workers.[39,40]

The hypothesis that PSHQ6−12 is flow-aligning implies that the evolution of macroscopic orientation, and the associated mechanical stresses, might be understood in straightforward terms given the simplicity of the underlying dynamic response in a single "domain". In the following section, we adopt a very simple modeling approach to seek additional insights into these data on PSHQ6−12.

4. Simulations: Polydomain Ericksen Model Calculations

4.1. Model Formulation. At shear rates sufficiently slow that the local molecular organization of the LCP is not significantly perturbed by flow, the linear continuum theory of Leslie and Ericksen[55] provides a complete description of nematic hydrodynamics and statics. We focus on the development of macroscopic orientation upon shear flow inception from an initially random polydomain state. Comprehensive modeling of LCP dynamics, even at low rates, presents formidable challenges. First, it is necessary to account for the distribution of director orientations in the textured material. Distortional elastic effects will influence the evolution of both structural and rheological properties. Finally, the effect of flow on the disclination lines typically present in quiescent LCPs is largely unknown; progress has been made only in highly idealized geometries.[56]

Here, we consider the simplest possible description of orientation and stress evolution upon flow inception from a random polydomain. We account for the distribution of director orientation in textured samples, but assume that the orientation in each "domain" evolves independently. Distortional elastic effects are thus ignored in the structural evolution equations, as well as in the stress constitutive equation. The effects and fate of disclination lines are similarly neglected. These are drastic simplifying assumptions, but may be partially justified in considering flow-aligning LCPs. In this case, shear flow promotes a unique orientation toward which all domains ultimately evolve. In flow-aligning materials, distortional effects are largely confined to orientational boundary layers; given the comparatively high viscosity of LCPs, these boundary layers may have a minor influence on bulk properties at steady state. Still, it is unreasonable to expect quantitative predictions from this approach, and those elements of LCP behavior that cannot be predicted by this simple model are logically attributable to the neglected influence of distortional elasticity and/or defects.

Our simulations are based on Ericksen's transversely isotropic fluid model.[57] This model describes the time evolution of a single director in a flow field by the following equation:

$$\frac{\partial \mathbf{n}}{\partial t} = \mathbf{n}\cdot\mathbf{\Omega} + \lambda(\mathbf{n}\cdot\mathbf{D} - \mathbf{D}:\mathbf{nnn}) \tag{3}$$

where $\mathbf{D}$ is the rate of deformation tensor and $\mathbf{\Omega}$ is the vorticity tensor. The quantity λ, the tumbling parameter, indicates whether the material exhibits tumbling ($\lambda < 1$) or flow-aligning ($\lambda > 1$) behavior. When $\lambda < 1$, eq 3 is equivalent to the orientation evolution equation for a non-Brownian ellipsoidal particle, and tumbling dynamics are described by the well-known Jeffery orbits of suspension mechanics.[58] While it is possible to contrive rigid bodies that correspond to $\lambda > 1$,[59] this case has not received as much attention in the suspension literature. Since eq 3 is linear in velocity gradients, dynamics will scale with the applied strain independent of the deformation rate. The stress constitutive equation in Ericksen's model is

$$\tau = 2\mu\mathbf{D} + 2\mu_1\mathbf{D}:\mathbf{nnnn} + \mu_2(\mathbf{nn}\cdot\mathbf{D} + \mathbf{D}\cdot\mathbf{nn}) \tag{4}$$

where, following Larson,[60] we have neglected a term in Ericksen's original formulation that predicts an anisotropic stress in the absence of flow.

Our polydomain modeling assumes (i) each domain in an initially random distribution responds independently to the macroscopically applied shear rate, $\dot{\gamma}$, and (ii) bulk structural and rheological properties of the polydomain may be obtained by appropriate ensemble averages. To simulate a polydomain texture, eq 3 was used to compute director trajectories for an ensemble of 80 000 randomly generated initial orientations, and averaged quantities of interest were evaluated directly from these trajectories. For $\lambda < 1$, an analytical solution for the orientation distribution function was given by Okagawa, Cox, and Mason;[61] this was used to verify the accuracy of the algorithm employed here. For flow-aligning materials, the trajectory simulation approach maintains accuracy as the distribution becomes highly peaked near the flow-alignment angle, where use of an orientation distribution function would require finer and finer resolution, making it computationally difficult.

4.2. Orientation Development. The director orientation state may be characterized by a mesoscopic order parameter tensor, defined as[9]

$$\bar{\mathbf{S}} = \langle \mathbf{nn} \rangle - \mathbf{I}/3 \tag{5}$$

where $\mathbf{I}$ is the unit tensor and $\langle\cdots\rangle$ represents an average over the distribution of the director orientation. In our experiments, anisotropy is measured in the 1−3 plane, where "1" denotes the flow direction, "2" denotes the gradient direction, and "3" is the neutral direction. Hence, the appropriate metric of anisotropy is

$$\bar{S}_{11} - \bar{S}_{33} = \langle n_1^2 \rangle - \langle n_3^2 \rangle \tag{6}$$

For a random initial condition, this quantity will start at zero. Prolonged shear promotes uniform orientation at the flow-alignment condition, where $n_3 = 0$ and $n_1^2 = (\lambda + 1)/2\lambda$. Figure 7a shows the evolution of anisotropy in the director distribution function computed using various values of λ that predict flow-alignment. This measure of orientation grows monotonically as a function of applied shear strain to a final value, and at a rate that depends only on the assumed value of λ.

The results in Figure 7a may not be directly compared to bulk orientation measurements because they describe only the distribution of director orientation, while

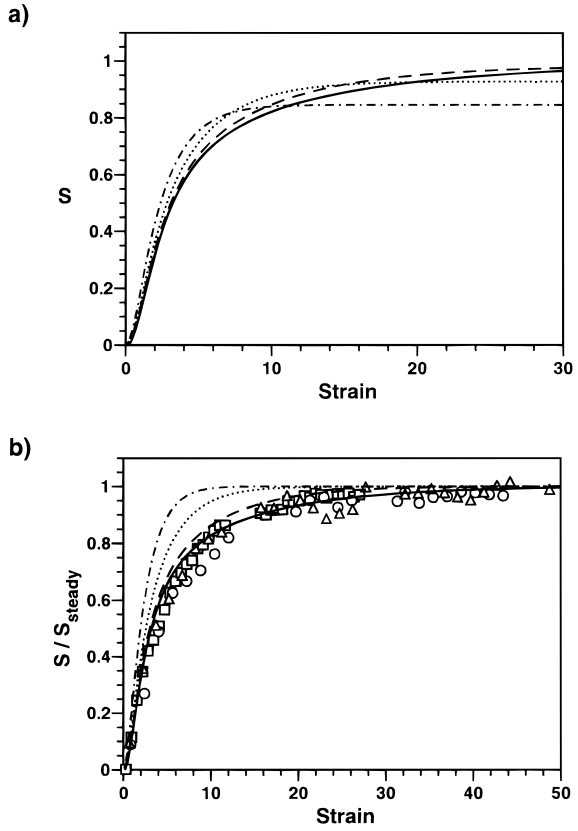

Figure 7. (a) Ericksen model simulations of anisotropy in the 1−3 plane during flow inception from a random polydomain initial condition, computed using $\lambda = 1.014$ (—), 1.035 (- - -), 1.167 (···), and 1.444 (—·—). (b) Computations from part (a), normalized by the steady-state value, compared to X-ray orientation data on PSHQ6-12.

experiments also reflect molecular level orientation (eq 1). Since it is assumed that S_m is unaffected by flow under conditions that allow use of linear continuum models, these calculations may be compared to experimental data by dividing by the steady-state anisotropy, as in Figure 5a. Figure 7b presents the results of such a comparison between the simple polydomain model and data, assuming flow alignment. Evidently, this modeling approach is able to predict the shape and strain scale of anisotropy development upon flow inception. When this procedure is repeated for various λ, a least-squares strategy shows that a value of $\lambda = 1.014$ best describes the experimental data over the strain range shown. The qualitative and quantitative success of this simple model lends further support to the hypothesis that PSHQ6−12 exhibits flow alignment.

4.3. Stress Predictions. For shearing flows, eq 4 may be used to predict the evolution of shear stress, τ_{12}, and first normal stress difference, $N_1 = \tau_{11} - \tau_{22}$, in terms of averages of director components evaluated from the strain-dependent distribution of director orientations:

$$\tau_{12} = \left[\mu + 2\mu_1\langle n_1^2 n_2^2\rangle + \frac{\mu_2}{2}\langle n_1^2 + n_2^2\rangle\right]\dot{\gamma} \qquad (7)$$

$$N_1 = 2\mu_1[\langle n_1^3 n_2\rangle - \langle n_1 n_2^3\rangle]\dot{\gamma} \qquad (8)$$

Both stresses scale linearly with shear rate.

To proceed, it is necessary to specify the relative magnitudes of the viscosity coefficients μ, μ_1, and μ_2. Apart from constraints to ensure thermodynamic consistency, a continuum theory makes no predictions of the phenomenological viscosity coefficients. Molecular models, however, do make specific predictions. Here, we consider two molecular models for LCPs that predict flow-alignment. The original Doi model for rodlike lyotropes invoked a mathematical approximation that leads to flow-alignment at low rates. Although this result is incorrect for both the model and for lyotropic LCPs, it may provide guidance about the signs and magnitudes of the Ericksen model viscosities. Linearization of the Doi model[62] leads to the following predictions:

$$\lambda = \frac{2 + S_m}{3S_m} \qquad (9a)$$

$$\frac{\mu}{\mu_1} = \frac{1}{3S_m + 2} \qquad (9b)$$

$$\mu_2 = -2\mu \qquad (9c)$$

The nematic dumbbell model of Maffettone and Marrucci[54] also predicts flow alignment and is more appropriate to the architecture of the model thermotropic LCP considered here. The model makes the assumption that local mesogen ordering is unaffected by flow, although chain stretching is allowed at a high Deborah number. In the low Deborah number limit, Ericksen model parameters may be extracted from the steady director and stress predictions of the nematic dumbbell model:[54]

$$\lambda = \frac{2 + S_m}{3S_m} \qquad (10a)$$

$$\frac{\mu}{\mu_1} = \frac{1 - S_m}{2 + S_m} \qquad (10b)$$

$$\mu_2 = -2\mu \qquad (10c)$$

Surprisingly, these two models differ only in their predictions of the relative magnitude of μ and μ_1, such that the middle term in eq 7 is of somewhat greater relative importance according to the nematic dumbbell model. Even this effect is only seen during transients, however. After prolonged shearing, uniform orientation of the director within the shear plane is predicted, with $n_1^2 + n_2^2 = 1$. This leads to cancellation of the terms involving μ and μ_2 in eq 7 according to both the linearized Doi and nematic dumbbell models. Indeed, this result occurs for any in-plane orientation state ($n_3 = 0$) and is closely related to the finding of Larson and Mead[63] that the Doi model predicts zero stress, but only rotation of the director when it is instantaneously parallel to either the flow or gradient direction. For these models, then, the ratio of N_1 to shear stress in steady-shear flow depends only on the flow-alignment angle, and thus on λ:

$$\frac{N_1}{\tau_{12}} = \frac{2}{\sqrt{\lambda^2 - 1}} \qquad (11)$$

Since λ and the μ_i all depend on S_m, it is possible to eliminate S_m and determine the value of μ/μ_1 which

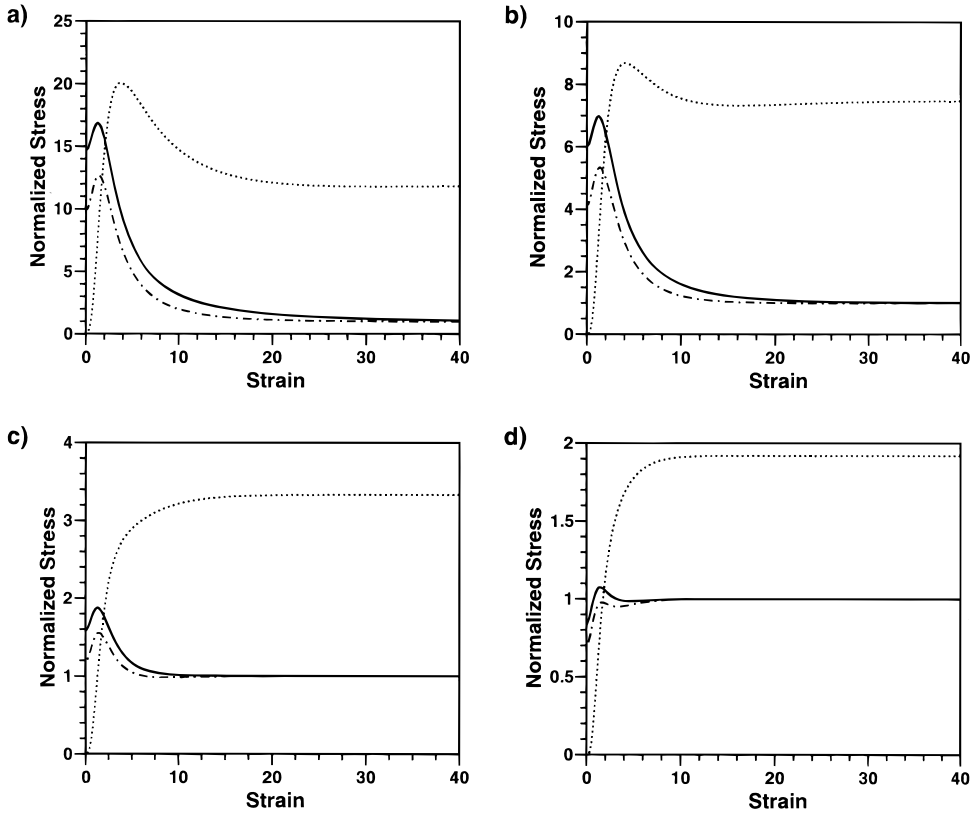

Figure 8. Ericksen model simulations of stresses during flow inception from a random polydomain initial condition. Stresses are normalized by steady-state shear stress. Shear stress computed using Ericksen viscosities predicted by the Doi model (—) and nematic dumbbell model (—•—); first normal stress difference predictions (•••) are the same for both models. Computations based on (a) $\lambda = 1.014$, (b) $\lambda = 1.035$, (c) $\lambda = 1.167$, and (d) $\lambda = 1.444$.

corresponds to a given λ using either the Doi or nematic dumbbell predictions.

Figure 8 presents polydomain Ericksen model predictions of shear and normal stresses during flow inception from a random polydomain, using the values of λ adopted in Figure 7, and corresponding Ericksen viscosities predicted by the Doi (eq 9) or nematic dumbbell (eq 10) models. All stresses are normalized by the steady-state shear stress. Comparing the Doi and nematic dumbbell predictions, only the transient shear stress is different, and the behavior is qualitatively similar in any case. Depending on the value of λ, both shear stress and first normal stress difference may or may not exhibit a significant stress overshoot during the transient approach to the flow-aligned condition. Generally, stress overshoots become more pronounced as λ approaches unity, corresponding to flow alignment closer and closer to the flow direction. This reflects a suppression of the steady-state stresses; using either Doi or nematic dumbbell predictions, the steady-state shear stress and first normal stress difference would disappear as n_2 approaches zero in the limit $\lambda \rightarrow 1$. For the isotropic initial distribution of director orientation, the odd moments appearing in eq 8 disappear, so N_1 is predicted to start at 0 upon flow inception. The shear stress, however, instantaneously jumps to a finite value, grows slightly to a maximum, and then evolves toward its steady-state value.

4.4. Discussion. Use of the Ericksen model should be most appropriate at steady state, where shear flow would promote homogeneous orientation in a flow-aligning nematic. Under these circumstances, shear stress and first normal stress difference should both scale linearly with the shear rate. In the shear rate range of 0.01−0.5 s^{-1}, Chang and Han observed behavior very close to these predictions in PSHQ6−12 at 160 °C,[37] although both shear stress and first normal stress difference grew somewhat less than linearly with the shear rate. Further, when either Doi or nematic dumbbell predictions of Ericksen viscosities are used, the steady-state ratio of N_1 to shear stress should be independent of shear rate, determined only by λ. At a shear rate of 0.1 s^{-1}, the data in Figure 5b approach a steady state in which $N_1/\tau_{12} = 7.6$, while a wider sample of Chang and Han's data[37] yields values in the relatively narrow range of 6.0−7.6 for shear rates between 0.01 and 0.5 s^{-1} at 160 °C. According to eq 11, this corresponds to values of λ in the range from 1.034 to 1.054.

Turning to the transient shear stress behavior upon flow inception from a random polydomain, these calculations seem capable of describing both the magnitude and duration of the shear stress overshoots typically seen in experiment (i.e., Figure 5b). In the polydomain modeling of Figure 8, transients reflect the development of macroscopic orientation, and stresses approach steady state around 10−20 strain units. This is in excellent agreement with the shear stress behavior in Figure 5b, and with transient shear stress data for a range of temperatures and shear rates presented by Chang and Han.[37] As seen in Figure 8, the magnitude of the shear stress overshoot normalized by the steady-shear stress is largely determined by the value of λ, when either Doi or nematic dumbbell predictions of Ericksen viscosities are used. A value of $\lambda = 1.035$, in the range suggested by the steady ratio of N_1 to shear stress, gives a peak-to-steady-shear stress ratio of 6.98 when Doi model parameters are used, and 5.34 when nematic dumbbell model parameters are used. At a shear rate of 0.1 s^{-1},

the data in Figure 5b yield an experimental value of 5.9 for PSHQ6−12 at 160 °C.

The self-consistency of this picture may be further tested by considering data of Chang and Han[37] at other temperatures. Their Figure 19 indicates that the ratio of N_1 to shear stress is essentially identical to that at 150 and 160 °C, which means an identical value of λ according to eq 11 exists. In this case, the ratio of peak-to-steady-state shear stress upon flow inception should also be the same. At 150 °C, the ratio is 5.3, quite close to the value of 5.9 observed at 160 °C. The polydomain Ericksen modeling thus seems to capture the essential characteristics of shear stress overshoots upon flow inception using parameters that are consistent with the steady-state ratio of N_1 to shear stress.

The transient behavior of the first normal stress difference seen in Figure 5b is *not* well-represented by these calculations. The magnitude of the N_1 overshoot is substantially larger than what is predicted using the range of λ adopted in Figures 7 and 8. Values of λ closer to 1 would yield transient overshoots of a larger magnitude; however, these would also lead to ratios of steady N_1 to shear stress that are much larger than those observed in PSHQ6−12. Another significant discrepancy is the duration of the transient. Experimentally, 100 or more strain units are required for N_1 to reach steady state, while the polydomain modeling predicts transients in the range of 10−20 strain units. Comparison of Figures 5a and 5b shows that the steady orientation state is firmly established well-before N_1 reaches its steady value. Taken together, these observations indicate that the transient response of N_1 is affected by physics missing from the simple polydomain modeling adopted here. Specifically, distortional elastic effects associated with deformation of disclination lines present in the polydomain sample probably contribute significantly to normal stresses measured during flow inception, and are the major contributing factor to the large stress overshoot observed experimentally.

Excepting the transient behavior of the first normal stress difference, several aspects of the observed experimental behavior (the development of macroscopic orientation, the steady ratio of N_1/τ_{12}, and the relative magnitude of shear stress overshoots) behave self-consistently when interpreted in terms of the polydomain Ericksen modeling used here. In all cases, values of λ close to 1 are suggested by comparisons between experiment and simulation. A somewhat smaller value of λ is necessary to describe the orientation development in Figure 7b as compared to the stresses. If one assumes that the ratio of N_1 to shear stress provides the correct λ (say, near 1.04), then Figure 7b implies that orientation development in the experiment is retarded somewhat relative to the polydomain model predictions. This might well be expected, in that any distortional elasticity would act to oppose the hydrodynamic torques rotating the director toward the flow-alignment condition.

Both the Doi and nematic dumbbell models predict that λ depends on molecular orientation in the same way (eqs 9a and 10a). According to these models, a value of $\lambda = 1.035$ requires a molecular order parameter $S_m = 0.95$. This is a very high degree of local ordering, and greatly exceeds the experimental measurements of the steady-state orientation parameter in Figure 3, which should represent only molecular ordering in a flow-aligning nematic. This discrepancy is likely due to two factors. First, these models are either of questionable applicability to model thermotropic LCPs (Doi), or of limited sophistication (nematic dumbbell), and hence cannot support the expectation of quantitative predictions of λ from the molecular order parameter. Second, it is likely that the results in Figure 3 understate the actual degree of mesogen ordering. The analysis embodied in eq 2 assumes that perfect mesogen ordering in a monodomain ($S_m = 1$) would result in an azimuthal intensity scan that gives a perfectly narrow peak at $\alpha = \pi/2$. While this may be a reasonable assumption for rigid rodlike lyotropic systems,[20] it is somewhat questionable given the architecture of the model thermotropic LCP considered here. Any additional spreading in azimuthal intensity due to the scattering properties of the individual mesogenic units leads to an underestimation of S_m. In any case, it is also important not to attribute too much significance to the λ values extracted by comparisons between experimental data and the Ericksen model simulations described here. It is preferable to perform direct measurement of λ using optical techniques on sheared monodomain samples;[26,64] such measurements on a wide range of thermotropic LCPs should be given high priority.

5. Conclusions

Quantitative measurements of molecular orientation have been performed using in situ X-ray scattering on the model thermotropic copolyester PSHQ6−12. The accessibility of the isotropic phase in this material allows well-defined initial conditions to be established for both rheological and structural measurements under shear. In comparison to previously published data on lyotropic LCPs, the rheological and structural behavior of PSHQ6−12 under shear is quite simple. No systematic dependence of orientation on the shear rate is seen in the nematic phase, although orientation does increase slightly with undercooling. Measurements of orientation during heating through the nematic−isotropic transition provide a direct illustration of how local ordering in the nematic phase results in a significant drop in viscosity. Upon cessation of shear flow within the nematic phase, essentially no change in orientation is seen for times of up to 1 h. This provides an explanation for the lack of significant stress overshoots previously reported for interrupted shear flow rheological tests on this material.[37] Upon flow inception from an initially random polydomain structure, orientation grows monotonically to its steady-state value in a process which scales with applied shear strain, accompanied by significant overshoots in shear stress and first normal stress difference. The sample becomes quite transparent under shear, although the loss in turbidity only occurs after flow has imparted significant net orientation.

All of these observations support the hypothesis that PSHQ6−12 is a flow-aligning nematic. The consequences of this hypothesis were further tested by polydomain simulations based on the Ericksen fluid model, in which the phenomenological viscosity coefficients were predicted by molecular models for LCPs. These simulations lead to many predictions that agree favorably with experiment. In particular, the steady ratio of first normal stress difference to shear stress, magnitude of shear stress overshoots, and development of macroscopic orientation in PSHQ6−12 could all be predicted using this model with reasonable self-consis-

tency. However, overshoots in the first normal stress difference observed experimentally are of greater magnitude and duration than what could be predicted using this model. This is attributed to a distortional elasticity associated with the deformation of disclinations in the polydomain sample. A comparison between experiment and simulations suggests a value of the tumbling parameter, λ, near 1.035 (i.e., predicting flow-alignment); however, direct measurements of λ using monodomain experiments should be attempted to confirm this hypothesis.

Acknowledgment. We gratefully thank Professor C. D. Han for providing the PSHQ6−12 sample used in this study and the rheological data that appears in Figures 3 and 5. Financial support was provided by a MURI project on Liquid Crystals sponsored by AFOSR. We thank David Cinader and Franklin Caputo for assistance with X-ray scattering measurements performed at the DuPont−Northwestern−Dow Collaborative Access Team (DND-CAT) Synchrotron Research Center located at Sector 5 of the Advanced Photon Source. DND-CAT is supported by the E.I. DuPont de Nemours & Co., the Dow Chemical Co., and the National Science Foundation through Grant DMR-9304725 and the State of Illinois through the Department of Commerce and the Board of Higher Education Grant IBHE HECA NWU 96. Use of the Advanced Photon Source was supported by the U.S. Department of Energy, Basic Energy Sciences, Office of Energy Research under Contract No. W-31-102-Eng-38. Finally, we thank Dow and DuPont for contributions toward the purchase of the Linkam Shearing Stage used in this work.

References and Notes

(1) Marrucci, G.; Greco, F. *Adv. Chem. Phys.* **1993**, *86*, 331.
(2) Kiss, G.; Porter, R. S. *J. Polym. Sci.: Polym. Phys. Ed.* **1980**, *18*, 361.
(3) Mewis, J.; Moldenaers, P. *Mol. Cryst. Liq. Cryst.* **1987**, *153*, 291.
(4) Larson, R. G.; Mead, D. W. *J. Rheol.* **1989**, *33*, 1251.
(5) Srinivasarao, M.; Berry, G. C. *J. Rheol.* **1991**, *35*, 379.
(6) Burghardt, W. R.; Fuller, G. G. *Macromolecules* **1991**, *24*, 2546.
(7) Yang, I. K.; Shine, A. D. *J. Rheol.* **1992**, *36*, 1079.
(8) Burghardt, W. R.; Fuller, G. G. *J. Rheol.* **1990**, *34*, 959.
(9) Larson, R. G.; Doi, M. *J. Rheol.* **1991**, *35*, 539.
(10) Doi, M. *J. Polym. Sci., Polym. Phys. Ed.* **1981**, *19*, 229.
(11) Kuzuu, N.; Doi, M. *J. Phys. Soc. Jpn.* **1984**, *53*, 1031.
(12) Marrucci, G.; Maffettone; P. L. *Macromolecules* **1989**, *22*, 4076.
(13) Larson, R. G. *Macromolecules* **1990**, *23*, 3983.
(14) Hongladarom, K.; Burghardt, W. R.; Baek, S. G.; Cementwala, S.; Magda, J. J. *Macromolecules* **1993**, *26*, 772.
(15) Hongladarom, K.; Burghardt, W. R. *Macromolecules* **1994**, *27*, 483.
(16) Hongladarom, K.; Secakusuma, V.; Burghardt, W. R. *J. Rheol.* **1994**, *38*, 1505.
(17) Burghardt, W. R. *Macromol. Chem. Phys.* **1998**, *199*, 471.
(18) Picken, S. J.; Aerts, J.; Visser, R.; Northolt, M. G. *Macromolecules* **1990**, *23*, 3849.
(19) Keates, P.; Mitchell, G. R.; Peuvrel-Disdier, E.; Riti, J. B.; Navard, P. *J. Non-Newtonian Fluid Mech.* **1994**, *52*, 197.
(20) Hongladarom, K.; Ugaz, V. M.; Cinader, D. K.; Burghardt, W. R.; Quintana, J. P.; Hsiao, B. S.; Dadmun, M. D.; Hamilton, W. A.; Butler, P. D. *Macromolecules* **1996**, *29*, 5346.
(21) Ugaz, V. M.; Cinader, D. K., Jr.; Burghardt, W. R. *Macromolecules* **1997**, *30*, 1527.
(22) Ugaz, V. M.; Cinader, D. K., Jr.; Burghardt, W. R. *J. Rheol.* **1998**, *42*, 379.
(23) Dadmun, M. D.; Han, C. C. *Macromolecules* **1994**, *27*, 7522.
(24) Walker, L. M.; Wagner, N. J. *Macromolecules* **1996**, *29*, 2298.
(25) Walker, L. M.; Kernick, W. A., III; Wagner, N. J. *Macromolecules* **1997**, *30*, 508.
(26) Srinivasarao, M.; Garay, R. O.; Winter, H. H.; Stein, R. S. *Mol. Cryst. Liq. Cryst.* **1992**, *223*, 29.
(27) Donald, A. M.; Windle, A. H. *Liquid Crystalline Polymers*; Cambridge University Press: Cambridge, 1992.
(28) Lin, Y. G.; Winter, H. H. *Macromolecules* **1991**, *24*, 2877.
(29) McCullagh, C. M.; Blackwell, J.; Jamieson, A. M. *Macromolecules* **1994**, *27*, 2996.
(30) Cocchini, F.; Nobile, M. R.; Acierno, D. *J. Rheol.* **1992**, *36*, 1307.
(31) Han, C. D.; Chang, S. *J. Rheol.* **1994**, *38*, 241.
(32) Han, C. D.; Chang, S.; Kimg, S. S. *Mol. Cryst. Liq. Cryst.* **1994**, *254*, 335.
(33) Kim, S. S.; Han, C. D. *J. Rheol.* **1993**, *37*, 847.
(34) Han, C. D.; Kim, S. S. *J. Rheol.* **1994**, *38*, 13.
(35) Han, C. D.; Kim, S. S. *J. Rheol.* **1994**, *38*, 31.
(36) Kim, S. S.; Han, C. D. *Macromolecules* **1993**, *26*, 6633.
(37) Chang, S.; Han, C. D. *Macromolecules* **1997**, *30*, 1656.
(38) Chang, S.; Han, C. D. *Macromolecules* **1997**, *30*, 2021.
(39) Baek, S.-G.; Magda, J. J.; Larson, R. G.; Hudson, S. D. *J. Rheol.* **1994**, *38*, 1473.
(40) Huang, C.-M.; Magda, J. J.; Larson, R. G. *J. Rheol.*, submitted for publication.
(41) Beekmans, F.; Gotsis, A. D.; Norder, B. *Rheol. Acta* **1997**, *36*, 82.
(42) Driscoll, P.; Masuda, T.; Fujiwara, K. *Macromolecules* **1991**, *24*, 1567.
(43) Beekmans, F.; Gotsis, A. D.; Norder, B. *J. Rheol.* **1996**, *40*, 947.
(44) Graziano, D. J.; Mackley, M. R. *Mol. Cryst. Liq. Cryst.* **1984**, *106*, 73.
(45) Alderman, N. J.; Mackley, M. R. *Faraday Discuss. Chem. Soc.* **1985**, *79*, 1.
(46) Gervat, L.; Mackley, M. R.; Nicholson, T. M.; Windle, A. H. *Philos. Trans. R. Soc. London, Ser. A* **1995**, *350*, 1.
(47) Romo-Uribe, A.; Windle, A. H. *Macromolecules* **1996**, *29*, 6246.
(48) Mather, P. T.; Romo-Uribe, A.; Han, C. D.; Kim, S. S. *Macromolecules* **1997**, *30*, 7977.
(49) Chang, S.; Han, C. D. *Macromolecules* **1996**, *29*, 2383.
(50) Mitchell, G. R.; Windle, A. H. In *Developments in Crystalline Polymers−2*; Bassett, D. C., Ed.; Elsevier: London, 1988; Chapter 3.
(51) Moldenaers, P.; Mortier, M.; Mewis, J. *Chem. Eng. Commun.* **1994**, *49*, 699.
(52) Greco, F.; Marrucci, G. *Liq. Cryst.* **1997**, *22*, 11.
(53) Semenov, A. N. *Sov. Phys. JETP* **1987**, *66*, 712.
(54) Maffettone, P. L.; Marrucci, G. *J. Rheol.* **1992**, *36*, 1547.
(55) Leslie, F. M. *Adv. Liq. Cryst.* **1979**, *4*, 1.
(56) Ryskin, G.; Kremenetsky, M. *Phys. Rev. Lett.* **1991**, *67*, 1574.
(57) Ericksen, J. L. *Arch. Ration. Mech. Anal.* **1960**, *4*, 231.
(58) Jeffery, G. B. *Proc. R. Soc., Ser. A* **1922**, *102*, 161.
(59) Bretherton, F. P. *J. Fluid Mech.* **1962**, *14*, 284.
(60) Larson, R. G. *Constitutive Models for Polymer Melts and Solutions*; Butterworth: New York, 1988; Chapter 10.
(61) Okagawa, A.; Cox, R. G.; Mason, S. G. *J. Colloid Interface Sci.* **1973**, *45*, 303.
(62) Marrucci, G. *Mol. Cryst. Liq. Cryst.* **1982**, *72*, 153.
(63) Larson, R. G.; Mead, D. W. *J. Rheol.* **1989**, *33*, 185.
(64) Mather, P. T.; Pearson, D. S.; Burghardt, W. R. *J. Rheol.* **1995**, *39*, 627.

MA981215K